Brain and Cognition 104 (2016) 15–24

Contents lists available at ScienceDirect

Brain and Cognition

journal homepage: www.elsevier.com/locate/b&c

Frequency tagging yields an objective neural signature of Gestalt formation

Nihan Alp [a,*], Naoki Kogo [a,1], Goedele Van Belle [b], Johan Wagemans [a], Bruno Rossion [b]

[a] Brain & Cognition, KU Leuven, Belgium
[b] Institute of Research in Psychology and Institute of Neuroscience, Université Catholique de Louvain, Louvain la Neuve, Belgium

ARTICLE INFO

Article history:
Received 12 May 2015
Revised 18 November 2015
Accepted 28 January 2016

Keywords:
Frequency tagging
Holistic perception
Illusory surface
Illusory contour
Gestalt formation

ABSTRACT

The human visual system integrates separate visual inputs into coherently organized percepts, going beyond the information given. A striking example is the perception of an illusory square when physically separated inducers are positioned and oriented in a square-like configuration (illusory condition). This illusory square disappears when the specific configuration is broken, for instance, by rotating each inducer (non-illusory condition). Here we used frequency tagging and electroencephalography (EEG) to identify an objective neural signature of the global integration required for illusory surface perception. Two diagonal inducers were contrast-modulated at different frequency rates f_1 and f_2, leading to EEG responses exactly at these frequencies over the occipital cortex. Most importantly, nonlinear intermodulation (IM) components (e.g., $f_1 + f_2$) appeared in the frequency spectrum, and were much larger in response to the illusory square figure than the non-illusory control condition. Since the IMs reflect long-range interactions between the signals from the inducers, these data provide an objective (i.e., at a precise and predicted EEG frequency) signature of neural processes involved in the emergence of illusory surface perception. More generally, these findings help to establish EEG frequency-tagging as a highly valuable approach to investigate the underlying neural mechanisms of subjective Gestalt phenomena in an objective and quantitative manner, at the system level in humans.

1. Introduction

The human visual system does not only extract information about the local properties of an image, but is also capable of combining all the information to construct a coherently integrated whole. In some cases, the integrated wholes are different than the sum of the parts (Wertheimer, 1923; for recent reviews, see Wagemans, Elder, et al., 2012; Wagemans, Feldman, et al., 2012). One of the well-known examples representing this holistic property of vision is the Kanizsa figure (Kanizsa, 1955). By placing inducers so that neighboring straight edges are aligned collinearly, a central illusory surface is perceived (Fig. 1A). This percept is accompanied by (1) an illusory lightness perception—the illusory surface appearing brighter than the background, (2) the perception of illusory contours in the gaps between the collinear inducer edges, together outlining the shape of the illusory surface, and (3) an illusory depth stratification—the illusory surface appearing to occlude the surrounding objects (and the inducers appearing as complete disks). By comparing it with a non-illusory variation of the figure, Kanizsa showed that the perception of an illusory surface reflects the global configuration of the image. Hence, it is a context-sensitive phenomenon. It is this property that makes the perception of this figure a true Gestalt phenomenon (Kogo & Wagemans, 2013).

The underlying neural mechanisms of the illusory surface perception have been first investigated in the non-human primate brain. von der Heydt, Peterhans, and Baumgartner (1984) showed that neurons in the secondary visual area (V2) of the monkey brain that are sensitive to luminance-defined boundaries also respond when illusory contours with the same orientation fall in their receptive field. Subsequent studies also showed neural responses corresponding to illusory contours in the Kanizsa figure in low level visual cortex (V1 and V2; Lee & Nguyen, 2001). This observation is important since it identifies neural activities corresponding to the subjective properties of perception, instead of merely reflecting the physical inputs. As a matter of fact, these neurons were activated by illusory figures but their responses were reduced significantly in non-illusory variations (Lee & Nguyen, 2001; Peterhans & von der Heydt, 1989; von der Heydt et al., 1984),

* Corresponding author.
E-mail address: Nihan.Alp@ppw.kuleuven.be (N. Alp).
[1] Shared first author.

http://dx.doi.org/10.1016/j.bandc.2016.01.008
0278-2626/

indicating that they are activated as a result of the global coherence of the local signals responding to the individual inducers.

Further single cell recording studies in monkeys, as well as scalp electroencephalography (EEG) and functional magnetic resonance imaging (fMRI) in humans have shown neural activities corresponding to the perception of an illusory surface at higher levels in the visual hierarchy (e.g., V4: Cox et al., 2013; V3, V4, V7, V8: Mendola, Dale, Fischl, Liu, & Tootell, 1999; lateral occipital complex (LOC): Murray et al., 2002; Stanley & Rubin, 2003). Populations of neurons in these areas are tuned to higher-order configurations and shapes, while the neurons active at illusory contours in V1 and V2 are tuned to the orientation of boundaries. Accordingly, it has been suggested that feedback projections from higher-level visual areas to lower-level areas are involved in illusory surface perception—the higher-level signaling the overall configuration of the image while the lower-level articulates the position and orientation of the illusory contours (Lee & Mumford, 2003; Stanley & Rubin, 2003). In this framework, the illusory surface emerges through inter-areal dynamic interactions in the hierarchy of visual cortex, responding to edges, computing border-ownership (figural side) and depth-order, constructing surfaces, and detecting shapes (Grossberg, 1994; Kogo, Strecha, Van Gool, & Wagemans, 2010; Kogo & Wagemans, 2013; Lee & Mumford, 2003; Stanley & Rubin, 2003). The neural activities that constitute illusory surface perception suggest that large-scale integration of neural signals is a key mechanism underlying the emergence of global, Gestalt-like properties (for reviews, see Lesher, 1995; Murray & Herrmann, 2013).

An important next step is to investigate how such global level integration is achieved. To do so, it is essential to go beyond increased signals in response to the Kanizsa figure, and identify an objective signature of neural activities underlying global integration, as indexed by the illusory surface perception. Importantly, this signature should be objectively dissociated from the neural response to the local elements forming the illusory percept. This issue can be tackled by the "frequency-tagging" approach obtained from EEG recorded on the human scalp. The frequency-tagging approach (Regan & Cartwright, 1970; Regan & Heron, 1969) takes advantage of the fact that presenting a periodic visual stimulus to the human brain leads to periodic responses directly related to the frequency of stimulation (the "steady state visual evoked potential", SSVEP, Regan, 1966; for a review, see Norcia, Appelbaum, Ales, Cottereau, & Rossion, 2015). This property allows the use of highly selective frequency markers that can define the signal objectively and precisely (i.e., the response to the stimulus at the experimentally-defined stimulation frequency). Moreover, the approach can be used to record responses from multiple, simultaneously presented stimuli "tagged" at different frequencies (i.e., "fundamental frequencies", which are the physically given frequencies to an image), and disentangle objectively their contribution to the brain's overall response (e.g., Andersen, Müller, & Hillyard, 2009; Appelbaum, Wade, Vildavski, Pettet, & Norcia, 2006; Boremanse, Norcia, & Rossion, 2013; Morgan, Hansen, & Hillyard, 1996; Regan & Cartwright, 1970; Regan & Heron, 1969; Regan & Regan, 1988).

Of particular interest for the present purpose are frequency components that are not present in the input but correspond to nonlinear combinations of these frequency inputs (Regan & Regan, 1988; Zemon & Ratliff, 1984). For example, if two fundamental frequencies f_1 and f_2 are applied to two separate elements in an image, responses at frequencies such as $f_1 + f_2$, or $f_1 - f_2$ ($nf_1 \pm mf_2$, in general, with n and m being any positive integers) may be observed. These responses are referred to as "intermodulation components" (IMs, Zemon & Ratliff, 1984). The emergence of these frequencies cannot be explained by an independent modulation by the individual frequencies given in the input, but only as the result of non-linear responses of the system to the interactions of fundamental frequencies (Regan & Regan, 1988; Zemon & Ratliff, 1984). These properties of IMs suggest that this approach is ideal to objectively record neural activities that correspond to the *emergence* of a holistic representation, i.e. a representation that goes beyond the physically given stimulus by causing new frequency components in the frequency spectrum, and that can be objectively separated from the responses to the stimulus elements.

Although the EEG frequency-tagging combined with the analysis of IMs is not a new technique, its significance in investigating the neural basis of Gestalt-like visual integration has been realized relatively recently and only in a handful of studies. For instance, this approach has been used to investigate the neural basis of spatial integration in Vernier stimuli (Victor & Conte, 2000), to detect contextual effects in orientation-sensitive neural responses (Hou, Pettet, Sampath, Candy, & Norcia, 2003), and of interactions between a figure and its background (Appelbaum, Wade, Pettet, Vildavski, & Norcia, 2008). Recent studies have also shown that the IMs generated by two halves of a face directly correlate with the integration of the two halves into a coherent percept of the face (Boremanse, Norcia, & Rossion, 2014; Boremanse et al., 2013). Hence, these studies indicate that populations of neurons whose receptive fields cover the nearby elements with the two different frequencies, such as the two neighboring line segments in the Vernier stimuli, or figure and ground regions that abut at a boundary or two face halves, can create IMs. Importantly, a study on motion binding (Aissani, Cottereau, Dumas, Paradis, & Lorenceau, 2011) also reported IMs when the two frequency tags were assigned to elements that are physically distant in the image (see also Fuchs, Andersen, Gruber, & Müller, 2008; Gundlach & Müller, 2013). Therefore, IMs can also arise from long-range interactions between populations of neurons that represent retinotopically distal elements.

These recent developments suggest that applying EEG frequency-tagging with the IM signal analysis can provide an objective signature of the emergence of Gestalt-like properties as the result of global integration. Here, as a representative example of a holistic, Gestalt-like phenomenon, we investigate the IM signals corresponding the illusory surface perception in the Kanizsa figure. Since the illusory surface is assumed to result from the coherent integration of the locally triggered neural signals, long-range neural interactions should generate IM components. In fact, a recent study used two lateralized flickering stimuli (inducers) giving rise to an illusory surface perception, and reported IM components (Gundlach & Müller, 2013). The experimental stimulus in that study consists of three "incomplete" circles that give rise to a long horizontal illusory rectangle perceived to be in front of the three circles, a percept that is changed by completing the contour drawing of the central circle in the control stimulus (see Fig. 1a in that study). However, the control condition used in that study is somewhat ambiguous. In addition to giving rise to the (intended) percept of three separate shapes without any perceptual completion, it can also be perceived as perceptually completed, with a combination of modal and amodal completion. Specifically, the horizontal illusory rectangle is sometimes perceived (modal completion induced by the two peripheral circles) while being occluded by the central circle (amodal completion). To circumvent this problem, we rely here on Kanizsa's original square configuration and the standard non-illusory control (with rotated inducers) in the present study (Fig. 1), in which the perception of an illusory surface and its disappearance are well-established. Moreover, this previous study used relatively high frequency rates of stimulation (i.e., 8.5 Hz and 14.17 Hz). While such frequency rates generally provide robust SSVEPs, these responses are generally restricted to low-level visual areas such as the primary visual cortex, projecting to medial occipital sites (i.e. around electrode Oz), even when high-level visual stimuli are used (Alonso-Prieto et al., 2013; Bekthereva

& Müller, 2015). Furthermore, due to the lower temporal integration rate of high-level as compared to low-level visual areas, high-level differences, for instance between face identities (Alonso-Prieto et al., 2013) or images of different emotional valence (Bekthereva & Müller, 2015) may be present with low (i.e., 6 Hz or less, as we used in our study: 2.94 Hz and 3.57 Hz) but not high frequency rates. Given that we are interested here in processes taking place in both low- and high-level visual areas, we used relatively low frequency rates of stimulation. To anticipate the remainder of this paper, we report that IMs over the occipital cortex are strongly enhanced in the illusory condition and we discuss the implications of the responses of the frequency components in terms of the neural activities involved in the emergence of the Gestalt-like phenomenon.

2. Materials and methods

2.1. Participants

Twenty-four healthy (11 males, age range; 19–25) undergraduate students from the University of Louvain (UCL) with normal or corrected-to-normal vision participated in the study. One of the participants' data was discarded from the analysis because of noisy data collection (no signal above noise at fundamental frequencies). Participants were naive to the goal of the experiment. They were paid 10 euros per hour for participation. Informed consent was provided before the experiment. The Biomedical Ethical Committee of UCL approved the experimental procedure.

2.2. Stimuli

In the experimental condition ("illusory condition (IC)"), four black inducers were placed on a white background to construct Kanizsa's illusory square figure (Fig. 1A). The size of the central square was 2.1° × 2.1° while the diameter of an inducer was 1.5° at a viewing distance of 100 cm. In the control condition ("non-illusory condition (NIC)"), the four inducers were rotated to break down the illusion (Fig. 1B). The angles of rotation in the non-illusory figure were (measured counterclockwise from the original orientations of the individual inducers in the illusory figure) 77° for the top-left, 82° for the top-right, 44° for the bottom-left, and 53° for the bottom-right inducers, respectively.

2.3. EEG frequency-tagging

The contrast of the two diagonal inducers was sinusoidally contrast-modulated at different frequencies from black to mid-gray (Fig. 1C). The reason to frequency-tag diagonal inducers was to counterbalance for any hemispheric dominance for one of the two fundamental frequencies. The two tagging frequencies, f_1 and f_2, were given to either the top-left to bottom-right pair and the top-right to bottom-left pairs, respectively, or vice versa. These two different ways of tagging are called "standard" and "opposite" tagging, respectively. In standard-tagging the top-left and bottom-right change at f_1 = 2.94 Hz and top-right and bottom-left change at f_2 = 3.57 Hz; in opposite-tagging the top-left and bottom-right change at f_2 = 3.57 Hz and top-right and bottom-left at f_1 = 2.94 Hz.

These specific frequency rates were chosen for the following reasons. First, relatively low frequency rates were selected in order to capture high-level visual processes as explained above, and were also based on studies using frequency-tagging with figure-ground stimuli (i.e., 3 Hz and 3.6 Hz, Appelbaum et al., 2006) reporting robust responses at these rates as well as intermodulation frequencies (Appelbaum et al., 2008). Second, the fundamentals, their harmonics and all possible IMs did not overlap. Third, both the fundamental frequencies and the sum of the fundamental frequencies fell outside of the range of alpha band (i.e., from 8 to 12 Hz) in order to maximize the signal-to-noise ratio (Regan & Regan, 1988). Finally, the exact values of the frequency rates were constrained by the refresh rate of the monitor (100 Hz) as they were obtained by dividing the refresh rate by integers; i.e., 100/28 = 3.57, 100/34 = 2.94.

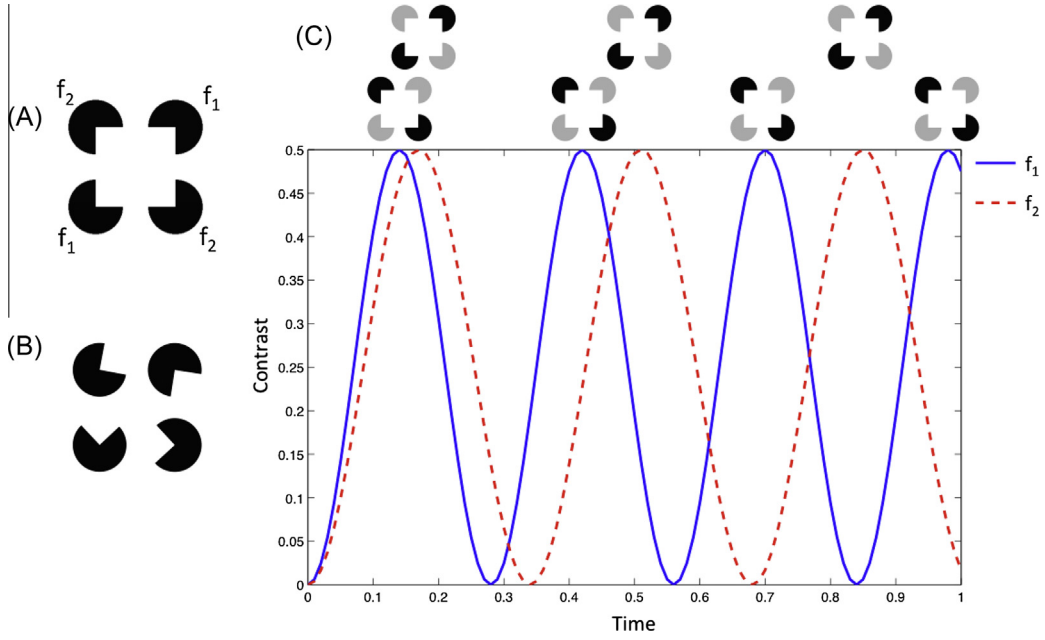

Fig. 1. (A) Kanizsa illusory surface. 4 inducers were placed in a way that gives rise to an illusory square at the center. (B) Non-illusory surface. Each individual inducer was rotated by a different angle to make the illusory surface at the center disappear (or at least diminish). (C) Schematic description of "*frequency tagging*". Two diagonal inducer pairs were tagged with two different frequencies. The example shows standard-tagging: top-left and bottom-right with f_1 = 2.94 Hz (red-dashed line); top-right and bottom-left with f_2 = 3.57 Hz (blue line). Contrast level of each pair changed from black to mid-gray. (For interpretation of the references to color in this figure legend, the reader is referred to the web version of this article.)

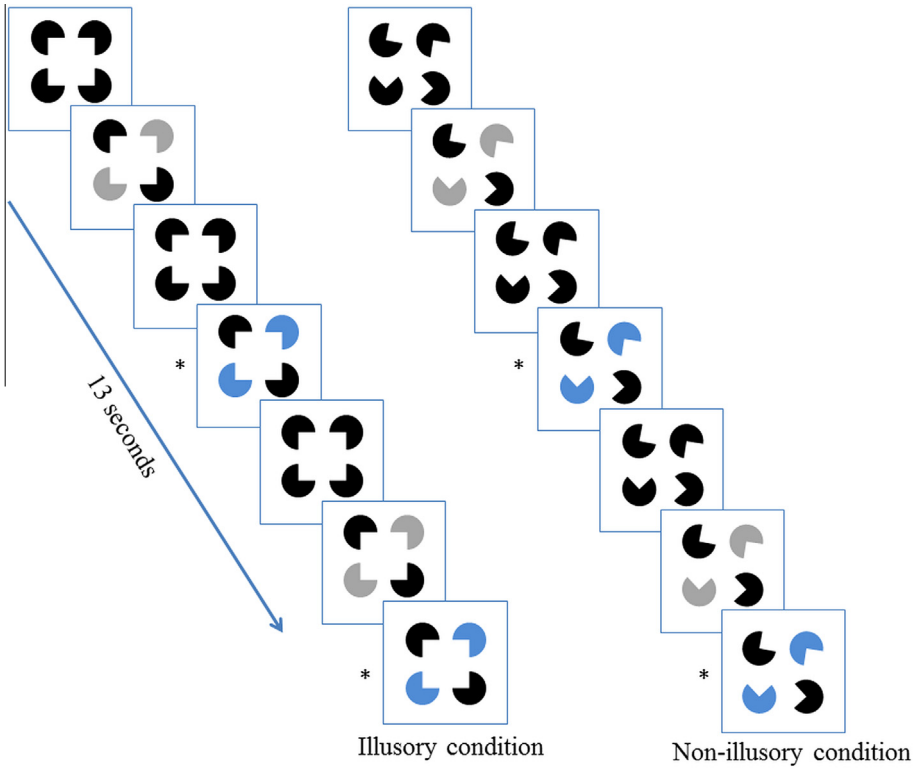

Fig. 2. Schematic illustration of experimental design of the study. The left side of the figure shows the experimental (illusory) condition and the right side shows the control (non-illusory) condition. Two diagonal inducer pairs flickered at different frequencies. Participants were asked to indicate the color change of the inducer pair from black to blue (indicated by asterisks). (For interpretation of the references to color in this figure legend, the reader is referred to the web version of this article.)

2.4. Procedure

After measuring the head size of each participant, the appropriate electrode cap (small, medium or large) was placed. Participants were seated in front of the display in a dimly lit room with viewing distance of 100 cm. Stimuli were displayed on a white background using an in-house application (SinStim) provided by UCL and written in Psychtoolbox (Brainard, 1997; Pelli, 1997) of MATLAB (MathWorks Inc., Natick, MA). Prior to the experiment, print-out versions of the stimuli were shown to the participants and they were asked to describe what they saw. Without any instructions, they all indicated the perception of the illusory surface in the experimental condition and the lack of it in the control condition. The experiment started with the presentation of a fixation cross in the middle of the screen, and then one of the two stimulus figures (illusory or non-illusory) was sinusoidally contrast-modulated for 13 s (Fig. 2).

Participants were asked to fixate the cross and spread their attention over the whole display all the time. At random times, two or four of the inducers briefly (300 ms) changed color to blue (0–4 changes within the trial; Fig. 2). Participants had to indicate the change of the color by pressing the "space" key of a keyboard. This orthogonal task was used to ensure that participants kept paying attention to the display during all trials. After approximately 8 s of interstimulus interval, the next trial was presented. Trials of the control and experimental conditions were randomized separately for each subject, while the counterbalanced assignments of f_1 and f_2 (standard and opposite tagging) were presented in separate blocks. Each condition was repeated 12 times ($2 * 12 = 24$ trials in total).

EEG activity was recorded using a BIOSEMI Active-Two amplifier system with 128 Ag/AgCl electrodes. Two additional electrodes (Common Mode Sense [CMS] active electrode and Driven Right Leg [DRL] passive electrode) were used as reference and ground electrodes, respectively. Vertical eye movements were recorded with two electrodes positioned above and below the right eyes. Horizontal eye movements were recorded with electrodes placed at the corner of each eye. EEG and electro-oculogram (EOG) recordings were sampled at 512 Hz.

3. Data analysis

EEG analysis was done by using Letswave 5 (http://nocions.webnode.com/letswave), Matlab (MathWorks Inc., Natick, MA) and EEGLAB (http://sccn.ucsd.edu). A two-pole Butterworth band-pass filter with cut-off frequencies at 0.3935 Hz and 39.8581 Hz was used to remove slow drift and high-frequency noise in the recording. The data were resampled to 250 Hz in order to reduce the workload and increase the speed of data processing. After filtering and resampling, the data were segmented into windows of 11.1076 s, containing exactly 7 cycles of $f_2 - f_1$ (0.63 Hz), the smallest IM component of interest (Bach & Meigen, 1999). Then, the data of all trials were averaged in the time domain within participants, separately for each condition, in order to increase the signal-to-noise ratio. FFT was performed to transform the data into the frequency domain, and the data were averaged between participants in the frequency domain for each condition. The frequency resolution of the EEG spectrum was 0.09 Hz (i.e., 1/11.1076). After FFT, Z-scores for each frequency component were computed using the mean and standard deviation of the ten neighboring frequency bins (5 on each side, excluding the first bin adjacent to the bin of interest (e.g., Liu-Shuang, Norcia, & Rossion, 2014), in order to determine which frequency components are significantly different from the noise level. Z-scores were first calculated based on the average of IC and NIC for the average of all channels and all

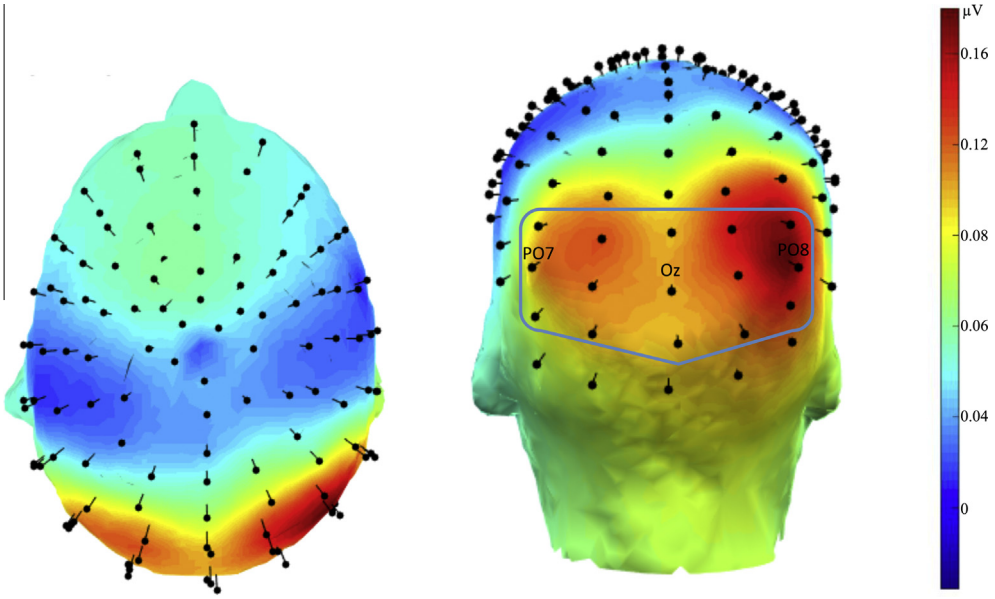

Fig. 3. Scalp topography of grand-averaged EEG responses across conditions for element-based responses. Both conditions, and all element-based responses, were averaged from all participants. The square indicates the 15 occipital electrodes that were selected for further analysis. (For interpretation of the references to color in this figure legend, the reader is referred to the web version of this article.)

participants, in order to determine the significant responses ($Z > 1.64$, $p < 0.05$ one-tailed, i.e. signal > noise) at the frequency components of interest and the intermodulation frequencies.

Next, to quantify the responses, we calculated average amplitude values of five neighboring bins on both sides, excluding the first bin adjacent to the bin of interest, and the amplitude at each frequency component was subtracted by this value to obtain the so-called "signal-to-noise subtraction" (hereafter called "SNS", see Dzhelyova & Rossion, 2014). This process was done for each electrode separately. SNS values of element-based responses (fundamentals and harmonics) and intermodulations (IMs), which survived *Z*-score significance, were averaged separately. The response at fundamental frequencies and harmonics was localized over the visual cortex, at medial and lateral occipital sites (Fig. 3). The fifteen contiguous medial and lateral occipital electrodes with the highest SNS values for the grand-averaged data across conditions were selected for further analysis (Fig. 3).

We focused on the six element-based responses (i.e., two fundamentals: $f_1 = 2.94$ Hz and $f_2 = 3.57$ Hz; four harmonics: $2f_1 = 5.88$ Hz, $2f_2 = 7.14$ Hz, $3f_1 = 8.82$ Hz, $3f_2 = 10.71$ Hz) and five intermodulations (IM components: $f_2 - f_1 = 0.63$ Hz, $2f_2 - f_1 = 4.20$ Hz, $f_1 + f_2 = 6.51$ Hz, $2f_1 + f_2 = 9.45$ Hz, $f_1 + 2f_2 = 10.08$ Hz), which survived *Z*-score calculation (see Table 1A for element-based responses and Table 1B for intermodulations).

Finally, to test the difference between the illusory and non-illusory conditions, a paired sample *t*-test (one-tailed: IC > NIC, according to hypotheses) was applied to the separate averages of six element-based responses and five intermodulation components.

Table 1A
Z-scores for element-based responses.

	Z-Score
f_1	2.0942
f_2	11.3673
$2f_1$	33.3173
$2f_2$	26.552
$3f_1$	10.2821
$3f_2$	6.1929

Table 1B
Z-scores for intermodulations.

	Z-Score
$f_2 - f_1$	2.0507
$2f_2 - f_1$	4.0332
$f_1 + f_2$	13.6
$2f_1 + f_2$	5.7796
$f_1 + 2f_2$	3.5255

4. Results

4.1. Element-based responses: fundamentals and their harmonics

As depicted in Fig. 4 (also see Table 2 for SNS and "signal-to-noise ratio" (SNR) values), the inducers elicited clear responses at the fundamental frequencies ($f_1 = 2.94$ Hz and $f_2 = 3.57$ Hz) and their harmonics (i.e., $2f_1 = 5.88$ Hz; $2f_2 = 7.14$ Hz, $3f_1 = 8.82$ Hz, $3f_2 = 10.71$ Hz), which were localized mainly over lateral and medial occipital electrodes (Fig. 3).

Overall, the element-based responses appeared slightly larger in the illusory condition than in the control condition (Fig. 5, left panel). Although this difference did not reach conventional levels of statistical significance, there was a trend (IC: 0.14 μV ± 0.05; NIC: 0.12 μV ± 0.05, $t = 1.94$, $p = 0.06$). When all of the components were tested individually for IC > NIC, none of them approached significance (Table 3A; all $p > 0.15$).

4.2. Intermodulation frequencies

Five IM components ($f_2 - f_1$, $2f_2 - f_1$, $f_1 + f_2$, $2f_1 + f_2$, $f_1 + 2f_2$) were significantly larger than noise level (see Table 1B). Statistical comparisons showed a significantly larger response for the illusory condition compared to non-illusory condition for the five IMs averaged together (see Fig. 5, right panel; IC: 0.07 μV ± 0.03; NIC: 0.05 μV ± 0.03, $t = 2.8$, $p = 0.01$). This effect was essentially due to two of the IMs, which were significantly larger in illusory than

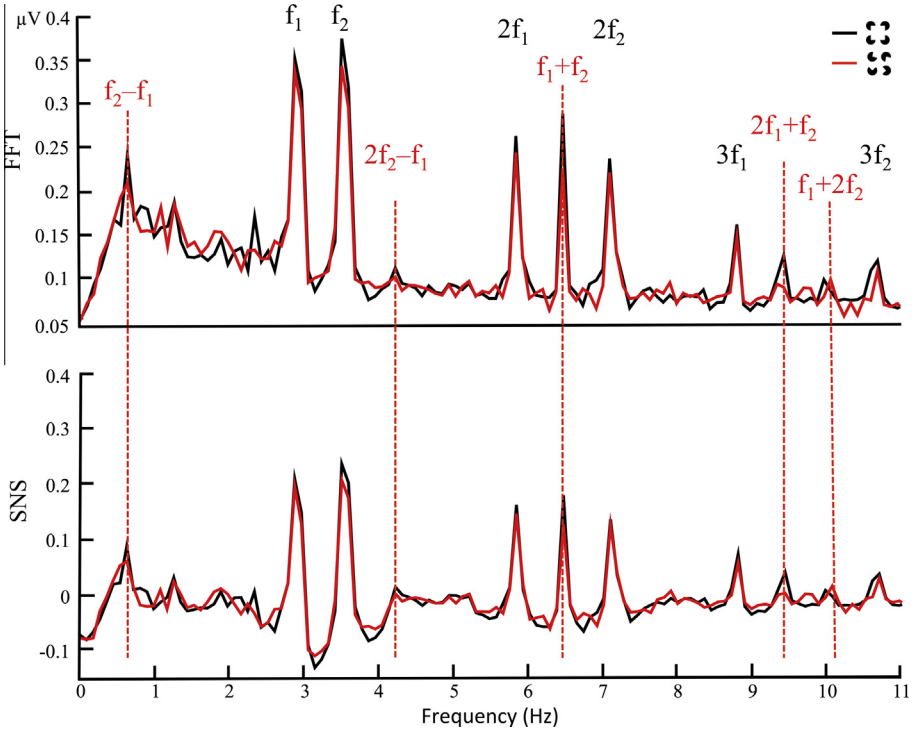

Fig. 4. EEG spectrum showing the different frequency components (averaged responses of fifteen occipital electrodes as illustrated in Fig. 3). The black line indicates the illusory condition (where all inducers were placed in a specific way so that they form a coherently integrated square at the center) and the red line indicates the non-illusory condition (where each individual inducer was rotated by a different angle to destroy the perception of illusory surface at the center). The upper plot represents FFT responses, while the lower plot indicates baseline-corrected (SNS) responses. Red dashed lines and frequencies that are marked with red font specify IM components, while frequencies that are marked with black font specify element-based responses. (For interpretation of the references to color in this figure legend, the reader is referred to the web version of this article.)

Table 2
SNS and SNR values of individual frequency components that survived *Z*-score criteria.

	SNS Values		SNR Values	
	IC	NIC	IC	NIC
$f_2 - f_1$	0.1009	0.0725	1.72	1.5349
f_1	0.16523	0.14326	2.1079	1.9598
f_2	0.2217	0.1925	3.2531	2.8692
$2f_2 - f_1$	0.0233	0.0104	1.2567	1.1148
$2f_1$	0.1796	0.1630	3.1154	3.0062
$f_1 + f_2$	0.1976	0.1420	3.1522	2.6824
$2f_2$	0.1523	0.1413	2.7834	2.7603
$2f_1 + f_2$	0.0515	0.0118	1.6866	1.1537
$3f_1$	0.0859	0.0692	2.1336	1.8861
$f_1 + 2f_2$	0.0061	0.0251	1.0706	1.3314
$3f_2$	0.0483	0.0402	1.6762	1.6088

non-illusory condition (Table 3B; $f_1 + f_2$: $t = 4.08$, $p = 0.0004$; $2f_1 + f_2$: $t = 2.67$, $p = 0.01$). Other IM components did not differ significantly between the conditions (Table 3B; all $p > 0.15$).

In addition, the difference in scalp topography between the two hemispheres was analyzed by comparing the six electrodes on the right and the six electrodes on the left. A repeated measure ANOVA with Greenhouse-Geisser correction (3-way ANOVA, right/left hemispheres, IC/NIC, element-based/IMs) was conducted. Results indicated that there was a significant difference between the two hemispheres in overall responses (i.e., right hemisphere dominance, $F(1.000, 22.000) = 6.72$, $p = 0.017$) but no interaction was found. To test further whether the generators of element-base and IM responses anatomically differ, individual FFT spectrum data for each condition were normalized. To calculate the normalized amplitude values, the value of each electrode was divided by scalp-wide root-mean square values (i.e., the square root of the sum of squares for all 128 electrodes) (McCarthy & Wood, 1985) for each participant. A repeated measure ANOVA with Greenhouse-Geisser correction (3-way ANOVA, 68 anterior and 60 posterior electrodes, IC/NIC, element-based/IMs) was conducted on these normalized amplitudes. The results revealed no main effect of IC/NIC, on both anterior $F(1.000, 22.000) = 0.018$, $p = 0.894$ and posterior electrodes $F(1.000, 22.000) = 0.042$, $p = 0.839$. The only significant interaction was between electrodes and element-based/IMs for anterior region $F(7.785, 171.276) = 2.719$, $p = 0.008$. The interaction between electrodes and element-based/IMs was significant on the posterior region $F(6.509, 143.194) = 9.917$, $p < 0.001$ as well as IC/NIC and electrodes $F(7.156, 157.427) = 2.060$, $p < 0.05$. The absence of a three-way interaction (Electrodes × IC/NIC × element-based/IMs) on both regions does not allow providing evidence for different neural generators for the differential response between illusory and non-illusory conditions for IMs and element-based responses.

Finally, for each participant, we subtracted out the response to NIC from the response to IC, separately for the element-based responses and the IMs. Two participants were discarded from the analysis (±2 standard deviations on one of the differentials measures). There was no significant correlation across the two differential measures ($r = 0.135$, $N = 21$, $p = 0.56$), suggesting further that the increase of the IMs in the illusory condition is not directly related to an increase to element-based responses.

5. Discussion

One of the advantages of EEG frequency-tagging technique is that neural signatures of interactions between elements can potentially be identified as emergent (non-linear) frequency components (IMs) that are distinct from the (fundamental) frequency tags given

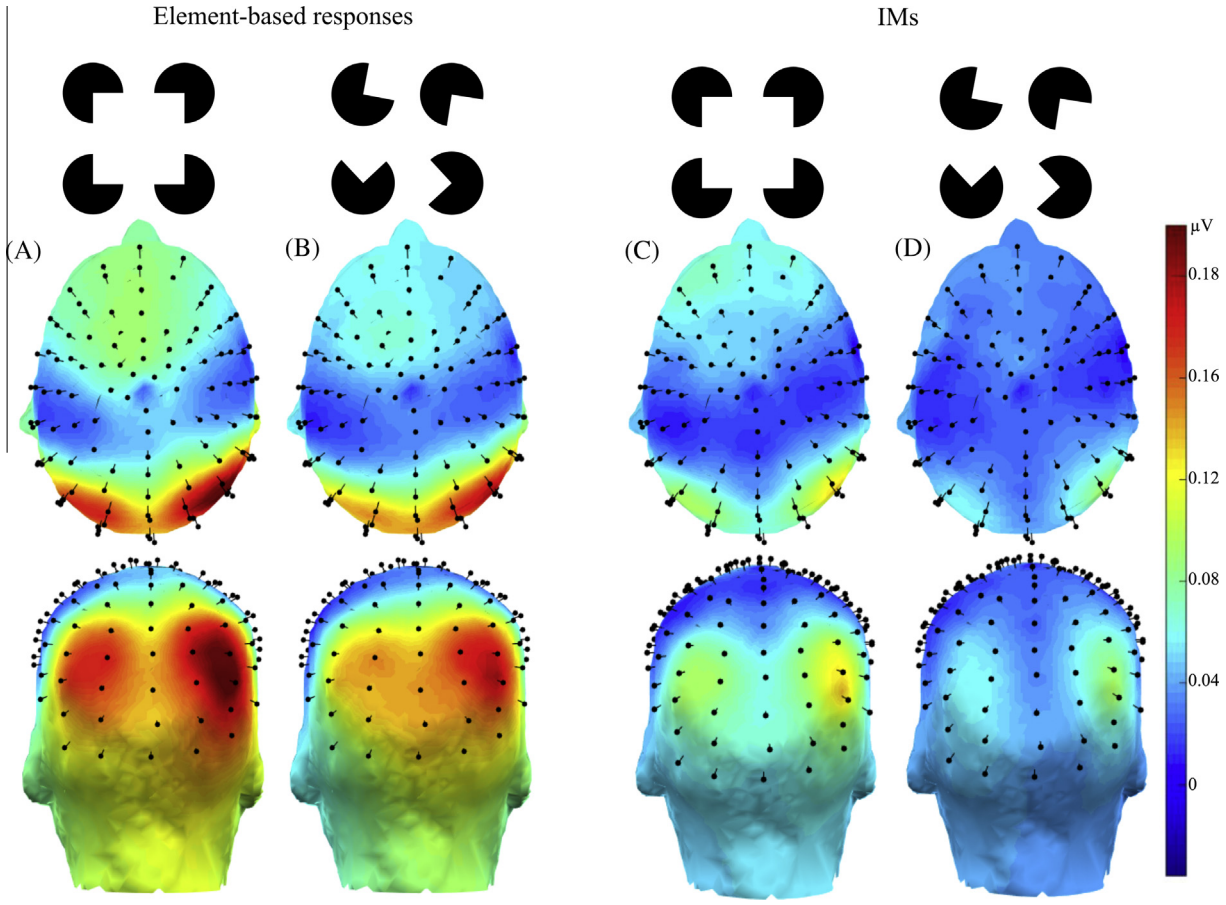

Fig. 5. Scalp topographies of baseline-corrected amplitude values for the six element-based responses averaged altogether and five intermodulation components averaged altogether. (A) Element-based responses for the illusory condition. (B) Element-based responses for the non-illusory condition. (C) IMs for the illusory condition. (D) Responses of IMs for the non-illusory condition. (For interpretation of the references to color in this figure legend, the reader is referred to the web version of this article.)

Table 3A
Mean (*M*), standard deviation (*SD*) and *p* values of fundamentals.

	IC		NIC		*T*-test	
	M	*SD*	*M*	*SD*	*t*(22)	*p*
Averaged fundamentals	0.14	0.05	0.12	0.05	1.94	0.06
f_1	0.16	0.11	0.14	0.11	0.94	0.35
f_2	0.22	0.1	0.19	0.13	1.29	0.2
$2f_1$	0.17	0.1	0.16	0.07	1.15	0.26
$2f_2$	0.15	0.08	0.14	0.09	0.88	0.38
$3f_1$	0.08	0.06	0.06	0.05	1.25	0.22
$3f_2$	0.048	0.04	0.04	0.04	1.04	0.3

Table 3B
Mean (*M*), standard deviation (*SD*) and *p* values of IMs.

	IC		NIC		*T*-test	
	M	*SD*	*M*	*SD*	*t*(22)	*p*
Average IMs	0.07	0.03	0.05	0.03	2.8	0.01
$f_2 - f_1$	0.1	0.11	0.07	0.09	1.17	0.25
$2f_2 - f_1$	0.04	0.07	0.03	0.07	0.44	0.66
$f_1 + f_2$	0.19	0.11	0.14	0.09	4.08	0.0004
$2f_1 + f_2$	0.052	0.05	0.011	0.03	2.67	0.01
$f_1 + 2f_2$	0.006	0.04	0.02	0.06	1.44	0.16

to the elements. The significantly larger IMs found in the responses to the Kanizsa figure compared to the non-illusory figure reported here indicate the non-linear interactions of neural activities underlying the emergent Gestalt properties in the perception of illusory surfaces.

5.1. IM components representing illusory surface perception

When the four inducers formed a specific configuration, giving rise to illusory surface perception, the IMs, considered altogether, were significantly larger in the illusory condition than in the non-illusory condition. Analysis of the individual IMs indicated that this effect was mainly driven by $f_1 + f_2$ and $2f_1 + f_2$. As IMs can emerge only when the two element-driven physically distal signals interact, the detection of IMs in the illusory condition constitutes direct evidence for long-range interactions of neural signals.

Our data showed that the differential responses between IC and NIC were different in different IM components. Mathematically, Fourier transformation of the result of a non-linear operation to the double sine waves, such as squaring or thresholding, gives exactly the same power at $f_2 - f_1$ and $f_1 + f_2$. What causes the different powers in different IMs is, we believe, the different frequency tunings of the various neuron types, the synapses, and the neural circuits involved in the processes of illusory surface perception. It is known that membranes of different neural subtypes have different resonance frequencies (Hutcheon & Yarom, 2000), so subtype-specific synaptic connections (Gupta, Wang, & Markram, 2000). In addition, neural circuits involved in processes with different complexity may show resonances at different frequencies. Kogo and colleagues hypothesized that border-ownership computation underlies the emergence of the illusory surface perception (Kogo & van Ee, 2015; Kogo & Wagemans, 2013; Kogo et al., 2010) while it is hypothesized that the border-ownership computation involves

a feedback circuit (Craft, Schutze, Niebur, & von der Heydt, 2007; Sugihara, Qiu, & von der Heydt, 2011; Zhou, Friedman, & von der Heydt, 2000). Hence, it is likely that the temporal dynamics of the feedback circuit contribute the pattern of IM responses. It is possible that the pattern of IM responses depends on where and how these inputs are processed with specific neural subtypes, synaptic connections, and neural circuit within and between hierarchical levels. In addition, the multi-stage processes would cause not only the emergence of $f_2 - f_1$ and $f_1 + f_2$ components – which do not correspond to specific visual events in the stimulus – but also the combinations of the harmonics of the fundamental frequencies such as $2f_1 + f_2$.

5.2. Fundamentals and harmonics representing the element-based responses

Even though element-based responses were slightly larger in the illusory condition than in the non-illusory condition (close to significance level), when averaged, none of the individual frequency components differed significantly between the two conditions. Furthermore, across individuals there was no relation between the differences in the element-based responses and the differences in the IMs. This suggests that the increase of IM components in the illusory condition is not related to changes in the representation of the elements. Therefore, our results indicate a clear distinction of neural responses represented by element-based and intermodulation components.

5.3. Comparison with previous work

Overall, our findings are in agreement with those of previous EEG frequency tagging studies that reported IMs during organized Gestalt percepts (Aissani et al., 2011; Gundlach & Müller, 2013). Aissani et al. (2011) asked observers to report their bound or unbound perception of vertical and horizontal moving bars arranged in a square shape, "frequency-tagged" at f_1 and f_2. In addition to occipital responses at f_1 and f_2, they found a specific IM $2f_1 + 2f_2$ that correlated with the perception of form/motion integration. However, this response was relatively weak and surprisingly localized in the medial part of the right precentral sulcus region. In terms of illusory surface perception, Gundlach and Müller (2013) observed IM components ($f_1 + f_2$ and $2f_1 + 2f_2$) that were larger when an illusory surface was intact rather than split in two parts and partially occluded, but the relation to illusory surface perception was not fully clear as noted in the introduction of the present paper. The differences in IMs that these authors reported could be explained by either the weaker illusory surface perception in the control condition or by the additional involvement of neural populations representing the perception of occlusion (Bushnell, Harding, Kosai, Bair, & Pasupathy, 2011; Kosai, El-Shamayleh, Fyall, & Pasupathy, 2014) as opposed to reflecting purely long-range interaction between two inducers that give rise to the illusory surface perception. Here we argue that in order to investigate the underlying mechanisms for illusory surface perception, it is essential that a control figure is clearly non-illusory. Using the classic Kanizsa figure and its non-illusory counterpart, our results provide unambiguous evidence for a much stronger IM activity over occipital sites during illusory as opposed to non-illusory surface perception.

In our study, the main difference between the illusory and non-illusory conditions appeared at the $f_1 + f_2$ and $2f_1 + f_2$ components. Some of these frequency components were absent in previous studies ($f_1 + f_2$ was absent in Aissani et al., 2011; $2f_1 + f_2$ was absent in both Aissani et al., 2011 and Gundlach & Müller, 2013). Moreover, when EEG frequency-tagging was applied to face stimuli, only the $nf_2 - mf_1$ ("difference IMs") reflected the binding properties of the two halves of a face, while the higher frequency "sum IMs" appeared to reflect the local low-level border interactions (Boremanse et al., 2013, 2014). The studies by Boremanse et al. used relatively low frequency stimulations (below alpha: 5.88 Hz and 7.14 Hz). An advantage of using lower frequency inputs is that they can reach higher levels of processing (Alonso-Prieto et al., 2013; Bekthereva & Müller, 2015; Zemon & Ratliff, 1984). This could be because the synchrony of lower frequency components is less disrupted, because of neural signals becoming more and more dispersive when they arrive at higher levels of processing, i.e. causing larger phase shift for high frequencies, or yet because of intrinsic longer integration times for complex stimuli in high-level visual areas than simple stimuli in low-level visual areas. Furthermore, the vulnerability of higher frequency signals to longer latencies of signal processing would also be a disadvantage for detecting feedback processes. While lower-level visual areas with feed-forward driven signals may be able to preserve the given frequency tag, the feedback projections from higher-level visual areas to lower-level areas with longer latencies may disturb the synchrony of the higher frequency signals more. This feedback might be critical for illusory surface perception, as discussed in the introduction, with the higher-level signaling the overall configuration of the image while the lower-level articulates the position and orientation of the illusory contours (Cox et al., 2013; Lee & Nguyen, 2001; Mendola et al., 1999; Murray et al., 2002; Stanley & Rubin, 2003). Thus, using lower frequency tags for elements as used here may help eliciting IM components. More generally, in future work, it will be important to clarify exactly what causes the differential neural responses between different IM components. This may shed light on why IM components that showed significant effects were different among the previous reports on Gestalt-like phenomena (Aissani et al., 2011; Appelbaum et al., 2008; Boremanse et al., 2013; Gundlach & Müller, 2013; Hou et al., 2003; Regan & Regan, 1988; Victor & Conte, 2000), with different experimental paradigms and choices of frequencies.

5.4. IM signals in non-illusory condition and element-based signals in illusory condition

Interestingly, responses to IM components were also found, albeit much weaker, in the non-illusory condition. This result indicates that long-range interactions can also occur without an emergent illusory surface perception. The population of neurons at the higher-level in the visual cortex with larger receptive fields may receive signals from some of the inducers with different tagging frequencies, and their responses may cause the emergence of the IM. Nevertheless, the fact that the IMs are larger in the illusory condition indicates that the long-range *coherent* interactions between local signals from inducers give rise to additional neural activities on top of the neural activities in the control condition, and this involves further non-linear processes in the neural circuit.

It is also important to compare the element-based frequency components between the illusory and non-illusory conditions. It is reasonable to assume that not only the neurons representing two inducers with two different tagging frequencies interact (between-pair interaction) but also the two inducers that are tagged with the same frequency may exhibit long-range interaction (within-pair interaction) in the illusory condition. The within-pair interaction may work to enhance the element-based responses. It is also possible that increased attention to the inducers may play a role in the illusory condition as a consequence of the task (pressing a space bar whenever two or four inducers change their color from black to blue). Attention not only alters the appearance of stimuli and increases contrast sensitivity (Carrasco, Ling, & Read, 2004), but may also modify the given frequency components. This attention effect depends on the figure-ground organization (Pei, Pettet,

& Norcia, 2002) and enhances the neurons representing the surfaces on the figural side (Qiu, Sugihara, & von der Heydt, 2007). The modification of neural activities depending on attention and figure-ground organization may be related to the element-based response. When the illusory surface is perceived, it is perceived as being in front of the surrounding four disks, which means that the four inducers are perceived as disks continuing behind the illusory surface. It should be noted, however, that a recent paper by Kok and de Lange (2014) reported that the fMRI BOLD signals in V1 representing inducers decreased in the illusory condition while the signals at the illusory surface region increased. The authors related this finding to the sharpening (specific enhancement of relevant signals) and error minimization (suppression of unnecessary signals) in the framework of predictive coding theory. In contrast, Cox et al. (2013) showed that neurons in V4 whose "focus of the receptive field" is within the inducers region did not show differential responses to illusory and non-illusory conditions. Hence, the detailed dynamics of the neural activities in the hierarchy of the visual cortex in illusory conditions need to be elucidated further by future research in terms of long-range and hierarchical interactions, attentional effects, and emergence of figure-ground organization.

5.5. Conclusions

Here, by contrasting the original Kanizsa figure with a non-illusory condition using frequency-tagging of the elements, we were able to objectively disentangle element-based and illusory-surface based activation at the neural level. That is, using a different frequency band than before, we were able to show objective neural signatures of long-range interactions during illusory surface perception, which were significantly larger than in the non-illusory condition. These findings also help to establish EEG frequency-tagging as a powerful technique to investigate the underlying neural mechanisms of subjective Gestalt phenomena in an objective and quantitative manner, at the system level in humans.

Acknowledgements

This work was supported by Fonds Wetenschappelijk Onderzoek – Vlaanderen (FWO-Flanders, PhD grant 11Q7314N to NA and post-doc grant 12L5112L to NK) a European Research Council (ERC, facessvep 284025) to BR, and long-term structural funding from the Flemish Government (METH/08/02 and METH/14/02) to JW. We also thank Talia Retter for technical help in data recording, Andrey Nikolaev for his help in analysis and very helpful discussions, and two anonymous reviewers for their careful reading and constructive comments on a previous version of this manuscript.

References

Aissani, C., Cottereau, B., Dumas, G., Paradis, A.-L., & Lorenceau, J. (2011). Magnetoencephalographic signatures of visual form and motion binding. *Brain Research, 1408*, 27–40.

Alonso-Prieto, E., Belle, G. V., Liu Shuang, J., Norcia, A. M., & Rossion, B. (2013). The 6Hz fundamental stimulation frequency rate for individual face discrimination in the right occipito-temporal cortex. *Neuropsychologia, 51*, 2863–2875.

Andersen, S. K., Müller, M. M., & Hillyard, S. A. (2009). Color-selective attention need not be mediated by spatial attention. *Journal of Vision, 9*, 1–7.

Appelbaum, L. G., Wade, A. R., Pettet, M. W., Vildavski, V. Y., & Norcia, A. M. (2008). Figure – ground interaction in the human visual cortex. *Journal of Vision, 8*(9), 1–19.

Appelbaum, L. G., Wade, A. R., Vildavski, V. Y., Pettet, M. W., & Norcia, A. M. (2006). Cue-invariant networks for figure and background processing in human visual cortex. *The Journal of Neuroscience: The Official Journal of the Society for Neuroscience, 26*(45), 11695–11708.

Bach, M., & Meigen, T. (1999). Do's and don'ts in Fourier analysis of steady-state potentials. Documenta Ophthalmologica. *Advances in Ophthalmology, 99*(1), 69–82.

Bekthereva, V., & Müller, M. M. (2015). Affective facilitation of early visual cortex during rapid picture presentation at 6 and 15 Hz. *Social Cognitive and Affective Neuroscience* (February 2013), 1–11.

Boremanse, A., Norcia, A. M., & Rossion, B. (2013). An objective signature for visual binding of face parts in the human brain. *Journal of Vision, 13*(11), 1–18.

Boremanse, A., Norcia, A. M., & Rossion, B. (2014). Dissociation of part-based and integrated neural responses to faces by means of electroencephalographic frequency tagging. *The European Journal of Neuroscience* (November 2013), 1–12.

Brainard, D. H. (1997). The psychophysics toolbox. *Spatial Vision, 10*, 433–436.

Bushnell, B. N., Harding, P. J., Kosai, Y., Bair, W., & Pasupathy, A. (2011). Equiluminance cells in visual cortical area v4. *The Journal of Neuroscience: The Official Journal of the Society for Neuroscience, 31*(35), 12398–12412.

Carrasco, M., Ling, S., & Read, S. (2004). Attention alters appearance. *Nature Neuroscience, 7*(3), 308–313.

Cox, M. A., Schmid, M. C., Peters, A. J., Saunders, R. C., Leopold, D. A., & Maier, A. (2013). Receptive field focus of visual area V4 neurons determines responses to illusory surfaces. *Proceedings of the National Academy of Sciences of the United States of America, 110*(42), 17095–17100.

Craft, E., Schutze, H., Niebur, E., & von der Heydt, R. (2007). A neural model of figure-ground organization. *Journal of Neurophysiology, 97*(6), 4310–4326.

Dzhelyova, M., & Rossion, B. (2014). The effect of parametric stimulus size variation on individual face discrimination indexed by fast periodic visual stimulation. *BMC Neuroscience, 15*(1), 87.

Fuchs, S., Andersen, S. K., Gruber, T., & Müller, M. M. (2008). Attentional bias of competitive interactions in neuronal networks of early visual processing in the human brain. *NeuroImage, 41*(3), 1086–1101.

Grossberg, S. (1994). Theory and evaluative reviews 3-D vision and figure-ground separation by visual cortex. *Perception and Psychophysics, 55*(1), 48–120.

Gundlach, C., & Müller, M. M. (2013). Perception of illusory contours forms intermodulation responses of steady state visual evoked potentials as a neural signature of spatial integration. *Biological Psychology, 94*(1), 55–60.

Gupta, A., Wang, Y., & Markram, H. (2000). Organizing principles for a diversity of GABAergic interneurons and synapses in the neocortex. *Science (New York, N.Y.), 287*(5451), 273–278.

Hou, C., Pettet, M. W., Sampath, V., Candy, T. R., & Norcia, A. M. (2003). Development of the spatial organization and dynamics of lateral interactions in the human visual system. *The Journal of Neuroscience: The Official Journal of the Society for Neuroscience, 23*(25), 8630–8640.

Hutcheon, B., & Yarom, Y. (2000). Resonance, oscillation and the intrinsic frequency preferences of neurons. *Trends in Neurosciences, 23*(5), 216–222.

Kanizsa, G. (1955). Margini quasi-percettivi in campi con stimolazione omogenea. *Rivista di Psicologia, 49*, 7–30.

Kogo, N., Strecha, C., Van Gool, L., & Wagemans, J. (2010). Surface construction by a 2-D differentiation–integration process: A neurocomputational model for perceived border ownership, depth, and lightness in Kanizsa figures. *Psychological Review, 117*(2), 406–439.

Kogo, N., & van Ee, R. (2015). Neural mechanisms of figure-ground organization: Border-ownership, competition and perceptual switching. In *Oxford handbook of perceptual organization* (pp. 352–372). Oxford: Oxford University Press.

Kogo, N., & Wagemans, J. (2013). The emergent property of border-ownership and the perception of illusory surfaces in a dynamic hierarchical system discussion paper the "side" matters: How configurality is reflected in completion. *Journal of Cognitive Neuroscience, 4*(1), 37–61.

Kok, P., & de Lange, F. P. (2014). Shape perception simultaneously up- and downregulates neuralactivity in the primary visual cortex. *Current Biology, 24*, 1531–1535.

Kosai, Y., El-Shamayleh, Y., Fyall, A. M., & Pasupathy, A. (2014). The role of visual area V4 in the discrimination of partially occluded shapes. *The Journal of Neuroscience: The Official Journal of the Society for Neuroscience, 34*(25), 8570–8584.

Lee, T. S., & Mumford, D. (2003). Hierarchical Bayesian inference in the visual cortex. *Journal of the Optical Society of America. A, Optics, Image Science, and Vision, 20*(7), 1434–1448.

Lee, T. S., & Nguyen, M. (2001). Dynamics of subjective contour formation in the early visual cortex. *Proceedings of the National Academy of Sciences of the United States of America, 98*(4), 1907–1911.

Lesher, G. W. (1995). Illusory contours: Toward a neurally based perceptual theory. *Psychonomic Bulletin and Review, 2*(3), 279–321.

Liu-Shuang, J., Norcia, A. M., & Rossion, B. (2014). An objective index of individual face discrimination in the right occipito-temporal cortex by means of fast periodic oddball stimulation. *Neuropsychologia, 52*, 57–72.

McCarthy, G., & Wood, C. C. (1985). Scalp distributions of eventrelated potentials: An ambiguity associated with analysis of variance models. *Electroencephalography and Clinical Neurophysiology, 62*, 203–208.

Mendola, J. D., Dale, a. M., Fischl, B., Liu, A. K., & Tootell, R. B. (1999). The representation of illusory and real contours in human cortical visual areas revealed by functional magnetic resonance imaging. *The Journal of Neuroscience: The Official Journal of the Society for Neuroscience, 19*(19), 8560–8572.

Morgan, S. T., Hansen, J. C., & Hillyard, S. A. (1996). Selective attention to stimulus location modulates the steady-state visual evoked potential. *Proceedings of the National Academy of Sciences of the United States of America, 93*(10), 4770–4774.

Murray, M. M., & Herrmann, C. S. (2013). Illusory contours: A window onto the neurophysiology of constructing perception. *Trends in Cognitive Sciences, 17*(9), 471–481.

Murray, M. M., Wylie, G. R., Higgins, B. A., Javitt, D. C., Schroeder, C. E., & Foxe, J. J. (2002). The spatiotemporal dynamics of illusory contour processing: Combined

high-density electrical mapping, source analysis, and functional magnetic resonance imaging. *The Journal of Neuroscience: The Official Journal of the Society for Neuroscience, 22*(12), 5055–5073.

Norcia, A. M., Appelbaum, G., Ales, J., Cottereau, B., & Rossion, B. (2015). The steady state visual evoked potential in vision research: A review. *Journal of Vision, 15*(4).

Pei, F., Pettet, M. W., & Norcia, A. M. (2002). Neural correlates of object-based attention. *Journal of Vision, 2*(9), 588–596.

Pelli, D. G. (1997). The VideoToolbox software for visual psychophysics: Transforming numbers into movies. *Spatial Vision, 10*, 437–442.

Peterhans, E., & von der Heydt, R. (1989). Mechanism of contour perception lines of pattern discontinuity visual Cortex II. *Journal of Neuroscience, 9*, 1749–1763.

Qiu, F. T., Sugihara, T., & von der Heydt, R. (2007). Figure-ground mechanisms provide structure for selective attention. *Nature Neuroscience, 10*(11), 1492–1499.

Regan, D. (1966). Some characteristics of average steady-state and transient responses evoked by modulated light. *Electroencephalography and Clinical Neurophysiology, 20*, 238–248.

Regan, D., & Cartwright, R. F. (1970). A method of measuring the potentials evoked by simultaneous stimulation of different retinal regions. *Electroencephalography and Clinical Neurophysiology, 28*, 314–319.

Regan, D., & Heron, J. R. (1969). Clinical investigation of lesions of the visual pathway: A new objective technique. *Journal of Neurology, Neurosurgery, and Psychiatry, 32*(5), 479–483.

Regan, M. P., & Regan, D. A. (1988). A frequency-domain technique for characterizing nonlinearities in biological-systems. *Journal of Theoretical Biology, 133*, 293–317.

Stanley, D. A., & Rubin, N. (2003). FMRI activation in response to illusory contours and salient regions in the human lateral occipital complex. *Neuron, 37*(2), 323–331.

Sugihara, T., Qiu, F. T., & von der Heydt, R. (2011). The speed of context integration in the visual cortex. *Journal of Neurophysiology, 106*(1), 374–385.

Victor, J. D., & Conte, M. M. (2000). Two-frequency analysis of interactions elicited by Vernier stimuli. *Visual Neuroscience, 17*(6), 959–973.

von der Heydt, R., Peterhans, E., & Baumgartner, G. (1984). Illusory contours and cortical neural responses. *Science, 224*, 1260–1262.

Wagemans, J., Elder, J. H., Kubovy, M., Palmer, S. E., Peterson, M., Singh, M., et al. (2012). A century of Gestalt psychology in visual perception: I. Perceptual grouping and figure-ground organization. *Psychological Bulletin, 138*(6), 1172–1217.

Wagemans, J., Feldman, J., Gepshtein, S., Kimchi, R., Pomerantz, J. R., van der Helm, P., et al. (2012). A century of Gestalt psychology in visual perception: II. Conceptual and theoretical foundations. *Psychological Bulletin, 138*(6), 1218–1252.

Wertheimer, M., 1923. *Untersuchungen zur Lehre von der Gestalt II*, Psychologische Forschung, 4, 301–350. Investigations on Gestalt principles (Michael Wertheimer, K. W. Watkins, Trans.). In Spillmann, L. (Ed.), 2012. *On perceived motion and figural organization* (pp. 127–182). Cambridge, MA: M.I.T. Press.

Zemon, V., & Ratliff, F. (1984). Intermodulation components of the visual evoked potential: Responses to lateral and suerimposed stimuli. *Biological Cybernetics, 50*, 401–408.

Zhou, H., Friedman, H. S., & von der Heydt, R. (2000). Coding of border ownership in monkey visual cortex. *Journal of Neuroscience, 20*(17), 6594–6611.